Supplementary Material

Metabolomic profiling and cytotoxic potential of three endophytic fungi of the genera *Aspergillus, Penicillium* and *Fusarium* isolated from *Nigella sativa* seeds assisted with docking studies

Nourhan Hisham Shady [a#] Jianye Zhang [b #] , Sara Khalid Sobhy [c, d] , Mohamed Hisham [e], Stefanie P. Glaeser [f], Faisal Alsenani [g], Peter Kämpfer [f], Mo'men H. El-Katatny [c] , Usama Ramadan Abdelmohsen [a,h]

[a] Department of Pharmacognosy, Faculty of Pharmacy, Deraya University, 61111 New Minia City, Minia, Egypt

[b] Guangzhou Municipal and Guangdong Provincial Key Laboratory of Molecular Target & Clinical Pharmacology, the NMPA and State Key Laboratory of Respiratory Disease, School of Pharmaceutical Sciences and the Fifth Affiliated Hospital, Guangzhou Medical University, Guangzhou 511436, China

[c] Department of Botany and Microbiology, Faculty of Science, Minia University, El-Minia 61519, Egypt.

[d] Faculty of Pharmacy, Deraya University, New Minia City, Minia, Egypt

[e] Department of Pharmaceutical Chemistry, Faculty of Pharmacy, Deraya University, New Minia City, Minia, Egypt.

[f] Institute of Applied Microbiology, Justus-Liebig University Gießen, Gießen, Germany.

[g] Department of Pharmacognosy, Faculty of Pharmacy, Umm Al-Qura University, Makkah 21955, Saudi Arabia

[h] Department of Pharmacognosy, Faculty of Pharmacy, Minia University, 61519 Minia, Egypt.

[*] Corresponding author: Department of Pharmacognosy, Faculty of Pharmacy, Minia University, Minia 61519, Egypt, usama.ramadan@mu.edu.eg

[#] Equal contribution

Abstract

The main aim of our study is to investigate the anticancer potential of our cultivated entophytic fungal strains from *Nigella sativa* seeds. The strains were identified by sequencing of the partial 18S rRNA gene and the internal transcribed spacer (ITS) region as *Aspergillus* sp. (SA4), *Penicillium* sp. (SA5), and *Fusarium* sp. (SA6). We carried out metabolic profiling for three fungal strains to investigate their metabolites diversity. Profiling of the different extracts revealed their richness in diverse metabolites and consequently fourteen compounds (**1–14**) were annotated. In addition, the obtained extracts were examined against three cell lines HepG2, MCF-7 and Caco-2 showed activity with IC_{50} values in the range of 1.95–39.7 μg/mL. Finally, molecular docking study was performed showing questinol as the lowest glide binding score value (-5.925 kcal/mol) among all identified compounds. Our results showed *Nigella sativa*-associated endophytes as a promising source for further studies to look for anticancer secondary metabolites.

Experimental

Plant material

Fresh plant seeds were collected from the Agricultural research center in Malawi, EL-Minia, Egypt. The investigated plant was identified by Prof. Nasser Barakat (Department of Botany and Microbiology, Faculty of Science, Minia University). A voucher specimen (NS- 1-2021) was conserved at Deraya University.

Isolation and identification of endophytic fungi

Isolation of endophytic fungi from seeds of *Nigella sativa* was carried out using the protocol by Strobel et al with slight modifications (Pavithra et al. 2012). *Nigella sativa* seeds were collected, rinsed with water followed by surface sterilization by 70% EtOH for 1 min, then washed with sterilized water followed by, 1.0% sodium hypochlorite (NaOCl) (v/v) for 1 min and finally with sterilized water. *Nigella sativa* seeds were crushed into small particles**.** Cultivation of the crushed seeds in a petri dish of dextrose agar medium- PDA (200 g potato, 20 g glucose, and 15 g agar in 1 L distilled water, Ph. 6.0) supplemented with 100 mg/L gentamycin and amoxicillin to suppress bacterial contamination. The Para film wrapped Petri dishes incubated at 28°C for 10 days in the incubator. The plates were examined daily for 10 days during the incubation period and any observation of growth of fungi were detected and isolated. Three strains, SA4, SA5 and SA6, were finally cultivated and isolated on the PDA medium and the isolates were maintained on plates for short-term storage and long-term strain collections in medium supplemented with 30% glycerol at −80 °C (Abdelmohsen et al. 2012). The endophytic fungi were transferred into a new agar slants and stored at 4°C for the further studies (Pharamat et al. 2013). Endophytes were deposited in the Microbial Repository of Botany and Microbiology (MRBM) Department, Faculty of Science, Minia University, Minia, Egypt, where they were stored at 4 °C.

Molecular identification and phylogenetic analysis

Phylogenetic identification of the isolated fungal strains recovered from the *Nigella sativa* seeds was achieved by DNA amplification and sequencing of partial 18S rRNA gene sequences and the fungal internal transcribed spacer (ITS) region (Sayed et al. 2020). Genomic DNA was extracted from fungal biomass harvested from agar plants MasterPure^{TM} Yeast DNA purification kit (epicentre, Illumina Company) after a mechanical treatment of the bacterial biomass (approx. 500 mg fresh weight) with 0.5 g

glass beats in the presence of 1 x PBS buffer pH 7.2, incubation with 1 ml of a 100 mg/ml lysozyme solution (in TE buffer, pH 8.0) at 37°C for 16 h), and an achromopeptidase treatment (60 U) at 37°C (30 min). Finally, the DNA was resolved in 40 µL pure water. The DNA quality and quantity were checked using NanoDrop spectrophotometer. Between 10 to 50 ng were used as DNA template per polymerase chain reaction (PCR) which were performed in a volume of 50 µL. The nearly full-length 18S rRNA gene and the adjacent ITS region including the ITS1, 5.8 S rRNA gene and ITS2 were amplified with the primer system NS1 (5′- GTAGTCATATGCTTGTCTC-3′) and ITS4 (5′-TTCCTCCGCTTATTGATATGC-3′) as described by Monchy et al (Monchy et al. 2011). The front part of the 18S rRNA genes was sequenced with primer NS1 and the complete ITS region with primer ITS4 according to White et al.(Innis et al. 2012). PCR product purification and sequencing reactions were performed by LGC Genomics (Berlin, Germany). Sequences were manually corrected based on the electropherogram using MEGA7 (Kumar et al. 2016). The corrected sequences were submitted to GenBank. The GenBank/EMBL/DDBJ Acc. numbers for the 18S rRNA gene and ITS sequences of strains SA4 to 6 are ON453995 to ON453997 and ON426964 to ON426966, respectively.

A first phylogenetic assignment based on the partial 18S rRNA gene and ITS region sequence (including ITS1, 5.8 S rRNA gene, and ITS2 sequences) was performed by BLASTn analysis against GenBank nucleotide sequence database and the internal transcribed spacer (ITS) from fungi type and reference strain databases provided in BLASTn tool of NCBI. The partial 18S rRNA gene sequences of the three strains were added to the SSU database SSURef NR 99 release 138.1 (12.06.2020) created by the SILVA project (Quast et al. 2012). Analysis in that database was performed with ARB version 6.0.4 (Ludwig et al. 2004)). The partial 18S rRNA gene sequences of the three fungal strains were aligned in the alignment explorer of ARB using the pt server built for the database by using the 10 next related sequences as references for the alignments. The aligned sequences were added to the database tree using the ARB parsimony (quick add marked) option without changing the overall tree topology. A partial tree with around 1514 reference sequences was exported.

Phylogenetic trees generated for ITS region sequences were generated in MEGA7. The 100 next related ITS sequences were downloaded from NCBI after BLAST analysis and aligned with the SA strain sequences using ClustalW implemented in MEGA7. A phylogenetic tree was calculated with the Maximum Likelihood method based on the

Kimura 2-parameter model (Kimura 1980) .Initial tree(s) for the heuristic search were obtained automatically by applying Neighbor-Join and BioNJ algorithms to a matrix of pairwise distances estimated using the Maximum Composite Likelihood (MCL) approach, and then selecting the topology with superior log likelihood value. A discrete Gamma distribution was used to model evolutionary rate differences among sites (5 categories (+G, parameter = 0,5089)). The rate variation model allowed for some sites to be evolutionarily invariable ([+I], 37,22% sites). The tree is drawn to scale, with branch lengths measured in the number of substitutions per site. The analysis involved 281 nucleotide sequences. All positions with less than 95% site coverage were eliminated. That is, fewer than 5% alignment gaps, missing data, and ambiguous bases were allowed at any position. There were a total of 391 positions in the final dataset.

Fermentation and extraction

Each isolated fungal endophyte, *Aspergillus* sp. SA4, *Penicillium* sp. SA5, and *Fusarium* sp. SA6, were fermented using the solid approach. In the solid treatment, 150 µL of each strain were inoculated and streaked on ten solid plates of the media: PDA (200 g potato, 20 g glucose, and 15 g agar in 1 L distilled water). The agar plates were cut into pieces and extracted with 300 mL of ethyl acetate (3 times) to get most of secondary metabolites produced during fermentation. Ethyl acetate was then evaporated using rotary evaporator (Heidolph ®, 35°C, 154 rpm) and the yielded dry extract was kept in refrigerator till further processing.

LC-MS Metabolomic analysis

Metabolomic profiling was performed on the crude fungal extracts on an Acquity Ultra Performance Liquid Chromatography system coupled to a Synapt G2 HDMS quadrupole time-of-flight hybrid mass spectrometer (Waters, Milford, CT, USA). Chromatographic separation was carried out on a BEH C18 column (2.1 × 100 mm, 1.7 µm particle size; Waters, Milford, CT, USA) with a guard column (2.1 × 5 mm, 1.7 µm particle size) and a linear binary solvent gradient of 0–100% eluent B over 6 min at a flow rate of 0.3 mL·min−1, using 0.1% formic acid in water (v/v) as solvent A and acetonitrile as solvent B. The injection volume was 2 µL and the column temperature was 40 ◦C. Ms converter software was used in order to convert the raw data into divided positive and negative ionization files. Obtained files were then subjected to the data mining software MZmine 2.10 (Okinawa Institute of Science and Technology Graduate University, Japan) for deconvolution, peak picking, alignment, deisotoping, and formula prediction. The

databases used for the identification of compounds were: MarinLit: http://pubs.rsc.org/marinlit/, and Dictionary of Natural Products (DNP) 2018: http://dnp.chemnetbase.com/faces/chemical/ChemicalSearch.xhtml.

Cytotoxicity Activity

The cytotoxic activity of different extracts of the three fungal strains SA4, SA5 and SA6 was tested against human hepatocellular carcinoma (HepG2), human breast cancer (MCF-7) and colon carcinoma (Caco-2) cell lines using MTT assay (Rasheed et al. 2017). We used doxorubicin as positive control. The cell lines were purchased from the American Type Culture Collection (Manassas, VA, USA). Cells were cultured using DMEM (Invitrogen/Life Technologies) supplemented with 10% FBS (Hyclone, USA), 10 µg/mL of insulin (Sigma), and 1% penicillin-streptomycin. Plate cells (cells density 1. 2 – 1.8 × 10,000 cells/well) were prepared in a volume of 100 µL complete growth medium with 100 µL of the tested sample per well in a 96-well plate for 24 hours before the MTT assay. MTT solution to be used was reconstituted with 3 ml of medium or balanced salt solution without phenol red and serum then it was added in an amount equal to 10% of the culture medium volume. Cultures were placed in incubator for 2-4 hours depending on cell type and maximum cell density (An incubation period of 2 hours is generally adequate but may be lengthened for low cell densities or cells with lower metabolic activity). After the incubation period, cultures were removed from incubator and the resulting formazan crystals were dissolved by adding an amount of DMSO equal to the original culture medium volume. Additionally, the absorbance of each plate was measured spectrophotometric ally at a wavelength of 570 nm using an ELISA plate reader (Model 550, Bio-Rad, USA). Three independent experiments were performed. IC_{50} values were determined as the concentration that produces 50% inhibition of the growth of cells and were calculated by GraphPad Prism 5 (Version 5.01, GraphPad Software, San Diego, CA, USA).

Results and discussion

Based on partial 18S rRNA gene sequences, strains SA4 and SA5 were identified as members of the family *Aspergillaceae* of the Ascomycota; Pezizomycotina; Eurotiomycetes; *Eurotiomycetidae*; Eurotiales and strain SA6 as member of the family of the *Nectriaceae* of the *Ascomycota*; *Pezizomycotina*; *Sordariomycetes*; *Hypocreomycetidae; Hypocreales*. A phylogenetic placement to next related *Aspergillus*

sp. and *Penicillum* sp. (SA4 and SA5) and *Fusarium* sp. (SA6) is illustrated based on partial 18S rRNA gene sequences in Figure A1 and based on the fungal ITS region sequences in Figure S2. To determine the chemical profiles of three strains, LC–MS-based metabolomics analysis was performed as shown in the total ion chromatograms Figure S3. The annotated-dereplicated compounds (Table S1, Figure S4) were identified by employing macros and algorithms that coupled MZmine with online and in-house databases, e.g. DNP and METLIN, in addition to the comparison with the reported literature data. Diverse chemical classes of metabolites were dereplicated such as polyketides, benzenoids, quinones and alkaloids. Identified compounds from strain SA4 were shown in (Table S1; Figure S4) including 4-hydroxybenzoic acid **(1)** that was dereplicated from the mass ion peak at *m/z* 138.03 in agreement with the molecular formula $C_7H_6O_3$, was reported to have HDAC inhibitory properties (Seidel et al. 2014). Moreover, the mass ion peak at *m/z* 164.046, consistent with the molecular formula $C_9H_8O_3$, was also identified as p-coumaric acid (**2**); *p*-coumaric acid is the abundant isomer of cinnamic acid and *p*-coumaric acid was reported to have antitumor and anti-mutagenic activities and its effect of *p*-coumaric acid against the colonic epithelial cells (Caco-2) was earlier studied (Jaganathan et al. 2013). Likewise, the mass ion peak at *m/z* 296.161 was annotated as ovalicin **(3)**; with the molecular formula $C_{16}H_{24}O_5$, This sesquiterpene compound was isolated from the fungus *Pseudorotium ovalis* and exhibited antitumor, and immunosuppressive activity ovalicin cytostatically inhibits the proliferation of endothelial cells (Griffith et al. 1997). Finally, the mass ion peak at *m/z* 488.231was dereplicated as cytochalasin Z **(4)** with the molecular formula $C_{29}H_{32}N_2O_5$ that produced by many fungal genera, including *Aspergillus* (Kushwaha et al. 2021).

On the other hand, metabolic profiling of the crude extracts of *Penicillium* sp. SA5 revealed a moderate number of metabolites (Table S1; Figure S4), of which the mass ion peak at *m/z* 230.078 in consonance with the molecular formula $C_{10}H_{14}O_6$ was also annotated as protulactone A **(6)**, It is a polyketide-derived fungal metabolite that has been isolated from an EtOAc extract of the marine-derived fungus *Aspergillus* sp. SF-5044 (Sohn and Oh 2010). Moreover, the mass ion peak at *m/z* 250.120, consistent with the molecular formula $C_{14}H_{18}O_4$, was also identified as aspergillumarin B **(10)**; that was reported from *Aspergillus* sp. (Tawfike et al. 2019).

Furthermore, metabolic profiling of the crude extracts of *Fusarium* sp. SA6 revealed a moderate number of metabolites (Table S1; Figure S4), the mass ion peak at *m/z* 284.06

with the molecular formula $C_{16}H_{12}O_5$ was also annotated as Viocristin **(12)**, this compound in ehrlich ascites carcinoma cells able to inhibit incorporation of uridine and thymidine. The incorporation of leucine was hardly effected (Anke et al. 1980). Moreover, peak at *m/z* 286.047, consistent with the molecular formula $C_{15}H_{10}O_6$ was annotated as Catenarin **(13)** (Jiang et al. 2016). Catenarin exhibited anti-proliferative activity towards the Caco-2 cell line (Al Kazman and Prieto 2021). Finally, the mass ion peak at *m/z* 300.062 was dereplicated as questinol **(14)**, with the molecular formula $C_{16}H_{12}O_6$ that was isolated from the broth extract of the fungus for the first time. Furthermore, it inhibited the production of pro-inflammatory cytokines, including IL-1β, TNF-α, and IL-6 and suppress the expression level of iNOS in a dose-dependent manner through the western blot analysis. Questinol might be selected as a promising agent for the prevention and therapy of inflammatory disease (Jin et al. 2016). The cytotoxic potential of the crude ethyl acetate extracts of the three endophytic fungi isolated from *Nigella sativa* seeds, *Aspergillus* sp. SA4*, Penicillium* sp. SA5 and *Fusarium* sp. SA6 were evaluated against three different cell lines (HepG-2, MCF-7, and Caco-2) using the MTT cell viability assay. Overall, the tested samples revealed varying *in vitro* growth inhibitory potencies against HepG-2, MCF-7, and Caco-2 tumor cells, showing IC_{50} values in the range of 1.95–39.7 µg/mL. As shown in Table S2, the extract of *Aspergillus* sp. SA4 cultured on PDA media exhibited the highest cytotoxicity against Caco-2 and HepG-2 cells, with IC_{50} value of 1.95 and 5.69 µg/mL, respectively, although it has moderate cytotoxicity against MCF-7 cells with IC_{50} value of 8.09 µg/mL. Likewise, the extract of *Penicillium* sp. SA5 cultured on the PDA medium, showed highest activities against the Caco-2 cell line, with IC_{50} values of 5.78 µg/mL but has weak activity against HepG-2 and MCF-7 with IC_{50} value of 39.7 and 22.7 µg/mL respectively. In contrast, the extract of *Fusarium* sp. SA6 cultured on PDA medium show cytotoxic effects against MCF7 cells (IC_{50}= 3.13µg/mL), while it has moderate activity with Caco-2 cell line with IC_{50} value of 10.4 µg/mL and weak activity against HepG-2 cells with IC_{50} value of 16.9 µg/mL. However, all the above-mentioned extracts showed higher cytotoxic potential as compared to the positive control, *staurosporine* that revealed IC_{50} values of 8.7, 6.67, and 8.05 µg/mL in the case of HepG-2, MCF-7, and Caco-2 cells, respectively (Table S2). To analyze the significant antiproliferative effect of isolated compounds from *Aspergillus* sp. SA4, *Penicillium* sp. SA5 and *Fusarium* sp. SA6, the X-ray crystal structure of human Su(var)3–9, enhancer of Zeste, Trithorax (SET)/inhibitor 2 of protein phosphatase 2A (I2PP2A) oncoprotein; (PDB: 2E50) (Shady et al. 2021) was selected for molecular modeling studies using

computational program Schrödinger Small Drug Discovery Suite 2021-2 software (Hisham et al. 2022).

SET is a multifunctional oncoprotein that plays a role in cell cycle progression, cell migration, apoptosis, transcription, and DNA repair, among other things (Gadallah et al. 2022). Overexpression of SET oncoprotein contributes to cancer progression (which is also known as an inhibitor to tumor suppressor protein phosphatase 2 A (PP2A) (Gadallah et al. 2022). As a result, inhibiting SET would serve a significant and effective role in inhibiting the growth of cancerous cells. D-erythro(e)-C18 ceramide was used as a flexed ligand in induced fit docking because to its better affinity for binding to SET protein (De Palma et al. 2019). The glide scores of compounds isolated from endophytic fungi species against the SET oncoprotein active site are summarized in **Table S3**. From the data presented in the table, fortunately all isolated compounds' glide score value is higher than reference D-e-C18 ceramide. The docked analysis of D-e-C18 ceramide indicated a good glide score (-3.627 kcal/mol) and glide energy (-53.69 kcal/mol), with three hydrogen bond interactions: two hydroxyl groups forms hydrogen bond interaction via Glu 111 and Gln 65 amino acid residue (1.92 and 1.96 Å, respectively). The third one via Thr 113 amino acid residue and NH group (1.88 Å) of D-e-C18 ceramide **Figure S5.**

Questinol showed the lowest glide binding score value (-5.925 kcal/mol) among all isolated compounds. It revealed four hydrogen bond interaction through two hydroxyl groups via Glu 57 (1.71 Å) , Arg 64 (2.46 Å) and Glu 114 (1.92 Å) amino acid residues. Also, Oxygen atom of methoxy group formed H-bond with Trp 213 amino acid residue (1.87 Å). In addition, it had a hydrophobic contact via Arg 64 via the phenyl moiety of questinol (**Figure 1)**. Strain SA6 participated to have catenarin that has the lower glide energy among other isolated compounds and may possess their potent antiproliferative activity against HepG2, MCF7 and Caco-2. On other hand, catenarin has good glide score (-5.653 kcal/mol) and exhibit three hydrogen bond interactions through Glu 114 amino acid residue via hydroxyl group and Trp 213 amino acid residue via carbonyl group and hydroxyl group **Figure S6**.

Table S1. A list of the dereplicated metabolites from the investigated extracts of *Aspergillus* sp. SA4, *Penicillium* sp. SA5 and *Fusarium* sp. SA6.

No.	RT	Exact mass	Molecular formula	Name	References
Aspergillus sp. SA4					
1	2.55	138.030	$C_7H_6O_3$	4-Hydroxybenzoic acid	(Stott and Martin 1989)
2	2.85	164.046	$C_9H_8O_3$	*p*-Coumaric acid	(Hall 2001)
3	4.67	296.161	$C_{16}H_{24}O_5$	Ovalicin	(Cane and McIlwaine 1987)
4	4.75	463.2359	$C_{28}H_{33}NO_5$	Cytochalasin Z16	(Lin et al. 2009)
Penicillium sp. SA5					
5	3.96	322.105	$C_{16}H_{18}O_7$	8-Methoxy-1-naphthalenol-6-O-alpha-D-ribofuranoside	(Wu et al. 2018)
6	2.32	230.078	$C_{10}H_{14}O_6$	Protulactone A	(Lv et al. 2020)
7	3.67	152.046	$C_8H_8O_3$	3-Methoxy-2,5-toluquinone	(He et al. 2004)
8	3.59	224.151	$C_{12}H_2ON_2O_2$	3-Isobutyl-6-(1-hydroxy-2-methylpropyl)-2(1h)-pyrazinone	(Zhu 2018)
9	3.51	248.104	$C_{14}H_{16}O_4$	Aspergillumarin A	(Ying et al. 2021)

10	2.48	250.120	$C_{14}H_{18}O_4$	Aspergillumarin B	(Tawfike et al. 2019)
11	3.38	268.130	$C_{14}H_2OO_5$	Huaspenone B	(Ye et al. 2021)
Fusarium sp. SA6.					
12	4.56	284.067	$C_{16}H_{12}O_5$	Viocristin	(Brase et al. 2009)
13	3.68	286.047	$C_{15}H_{10}O_6$	Catenarin	(Youssef and Singab 2021)
14	3.77	300.062	$C_{16}H_{12}O_6$	Questinol	(Li et al. 2017)

270

Table S2: Cytotoxic activities of ethyl acetate extracts of strain SA4, strain SA5 and strain SA6.

Endophytic fungi	IC_{50} (µg/mL)		
	HepG2	MCF7	Caco2
SA4	5.69±0.27	8.09±0.39	1.95±0.09
SA5	39.7±1.89	22.7±1.08	5.78±0.28
SA6	16.9±0.81	3.13±0.15	10.4±0.5
Staurosporine	8.7±0.42	6.67±0.32	8.05±0.38

Table S3: Molecular docking results and interacting residues for compounds isolated from endophytic fungi species, D-erythro(e)-C18 ceramide within SET oncoprotein (pdb: 2E50) active site

Active site	Fungi	Compound	Glide score (kcal/mol)	Glide energy (kcal/mol)
SET oncoprotein Pdb: 2E50	SA4	**4-Hydroxybenzoic acid**	-5.522	-21.262
		***p*-coumaric acid**	-4.935	-22.847
		Ovalicin	-4.411	-31.977
		Cytochalasin Z	-3.055	-40.901
	SA5	**5-hydroxy-4-methoxynaphthalen-2-yl alpha-D-ribofuranoside**	-5.326	-52.537
		Protulactone A	-4.842	-32.444
		6-Methoxy-2-methyl-1,4-benzoquinone	-5.063	-22.672
		3-Isobutyl-6-(1-hydroxy-2-methylpropyl)-2(1*H*)-pyrazinone	-5.205	-33.443
		Aspergillumarin A	-5.872	-34.273
		Aspergillumarin B	-5.505	-33.720
		Huaspenone B	-4.112	-30.902
	SA6	**Viocristin**	-5.382	-35.004
		Catenarin	-5.653	-38.838
		Erythroglaucin	-5.512	-37.447
	D-erythro(e)-C18 ceramide		-3.627	-55.091

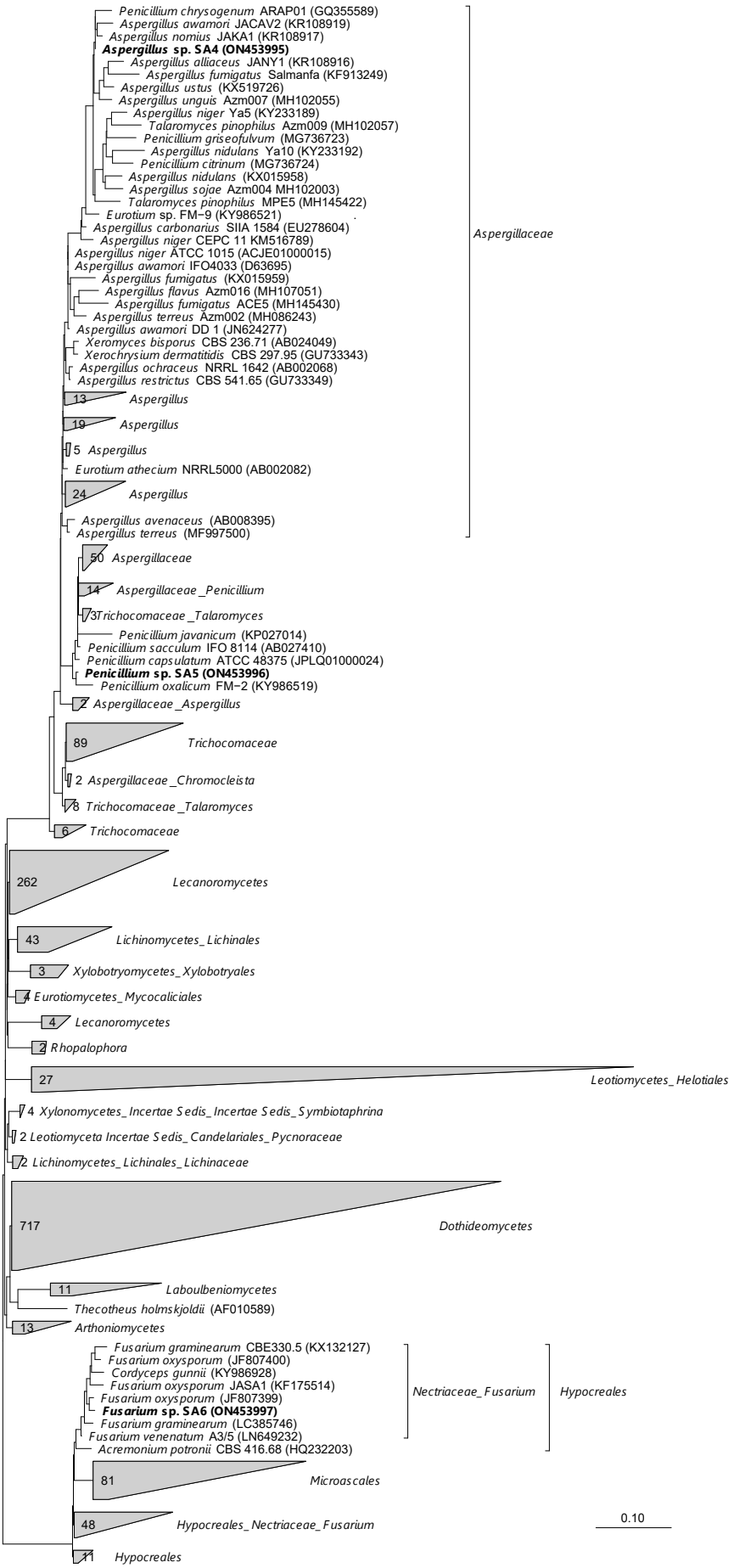
Penicillium chrysogenum ARAP01 (GQ355589)
Aspergillus awamori JACAV2 (KR108919)
Aspergillus nomius JAKA1 (KR108917)
Aspergillus sp. SA4 (ON453995)
Aspergillus alliaceus JANY1 (KR108916)
Aspergillus fumigatus Salmanfa (KF913249)
Aspergillus ustus (KX519726)
Aspergillus unguis Azm007 (MH102055)
Aspergillus niger Ya5 (KY233189)
Talaromyces pinophilus Azm009 (MH102057)
Penicillium griseofulvum (MG736723)
Aspergillus nidulans Ya10 (KY233192)
Penicillium citrinum (MG736724)
Aspergillus nidulans (KX015958)
Aspergillus sojae Azm004 MH102003)
Talaromyces pinophilus MPE5 (MH145422)
Eurotium sp. FM−9 (KY986521)
Aspergillus carbonarius SIIA 1584 (EU278604)
Aspergillus niger CEPC 11 KM516789)
Aspergillus niger ATCC 1015 (ACJE01000015)
Aspergillus awamori IFO4033 (D63695)
Aspergillus fumigatus (KX015959)
Aspergillus flavus Azm016 (MH107051)
Aspergillus fumigatus ACE5 (MH145430)
Aspergillus terreus Azm002 (MH086243)
Aspergillus awamori DD 1 (JN624277)
Xeromyces bisporus CBS 236.71 (AB024049)
Xerochrysium dermatitidis CBS 297.95 (GU733343)
Aspergillus ochraceus NRRL 1642 (AB002068)
Aspergillus restrictus CBS 541.65 (GU733349)
Aspergillus
Aspergillus
Aspergillus
Eurotium athecium NRRL5000 (AB002082)
Aspergillus
Aspergillus avenaceus (AB008395)
Aspergillus terreus (MF997500)
Aspergillaceae
Aspergillaceae_Penicillium
Trichocomaceae_Talaromyces
Penicillium javanicum (KP027014)
Penicillium sacculum IFO 8114 (AB027410)
Penicillium capsulatum ATCC 48375 (JPLQ01000024)
Penicillium sp. SA5 (ON453996)
Penicillium oxalicum FM−2 (KY986519)
Aspergillaceae_Aspergillus
Trichocomaceae
Aspergillaceae_Chromocleista
Trichocomaceae_Talaromyces
Trichocomaceae
Lecanoromycetes
Lichinomycetes_Lichinales
Xylobotryomycetes_Xylobotryales
Eurotiomycetes_Mycocaliciales
Lecanoromycetes
Rhopalophora
Leotiomycetes_Helotiales
Xylonomycetes_Incertae Sedis_Incertae Sedis_Symbiotaphrina
Leotiomyceta Incertae Sedis_Candelariales_Pycnoraceae
Lichinomycetes_Lichinales_Lichinaceae
Dothideomycetes
Laboulbeniomycetes
Thecotheus holmskjoldii (AF010589)
Arthoniomycetes
Fusarium graminearum CBE330.5 (KX132127)
Fusarium oxysporum (JF807400)
Cordyceps gunnii (KY986928)
Fusarium oxysporum JASA1 (KF175514)
Fusarium oxysporum (JF807399)
Fusarium sp. SA6 (ON453997)
Fusarium graminearum (LC385746)
Fusarium venenatum A3/5 (LN649232)
Acremonium potronii CBS 416.68 (HQ232203)
Nectriaceae_Fusarium
Hypocreales
Microascales
Hypocreales_Nectriaceae_Fusarium
Hypocreales
0.10

284

285 Figure S1 : Phylogenetic placement of the three fungal strains SA4, SA5 and SA6 based
286 on their partial 18S rRNA gene sequences. The sequences were aligned in ARB and
287 added to the database tree of the SSU database SSURef NR 99 release 138.1 (12.06.2020)
288 without changing the tree topology. Only a fraction of the tree is represented here
289 including 1574 sequences related to the SA strains. Numbers in clusters represent the
290 number of sequenced included in a cluster. Bar: 0.1 nucleotide substitutions per
291 nucleotide sequence positions.

292

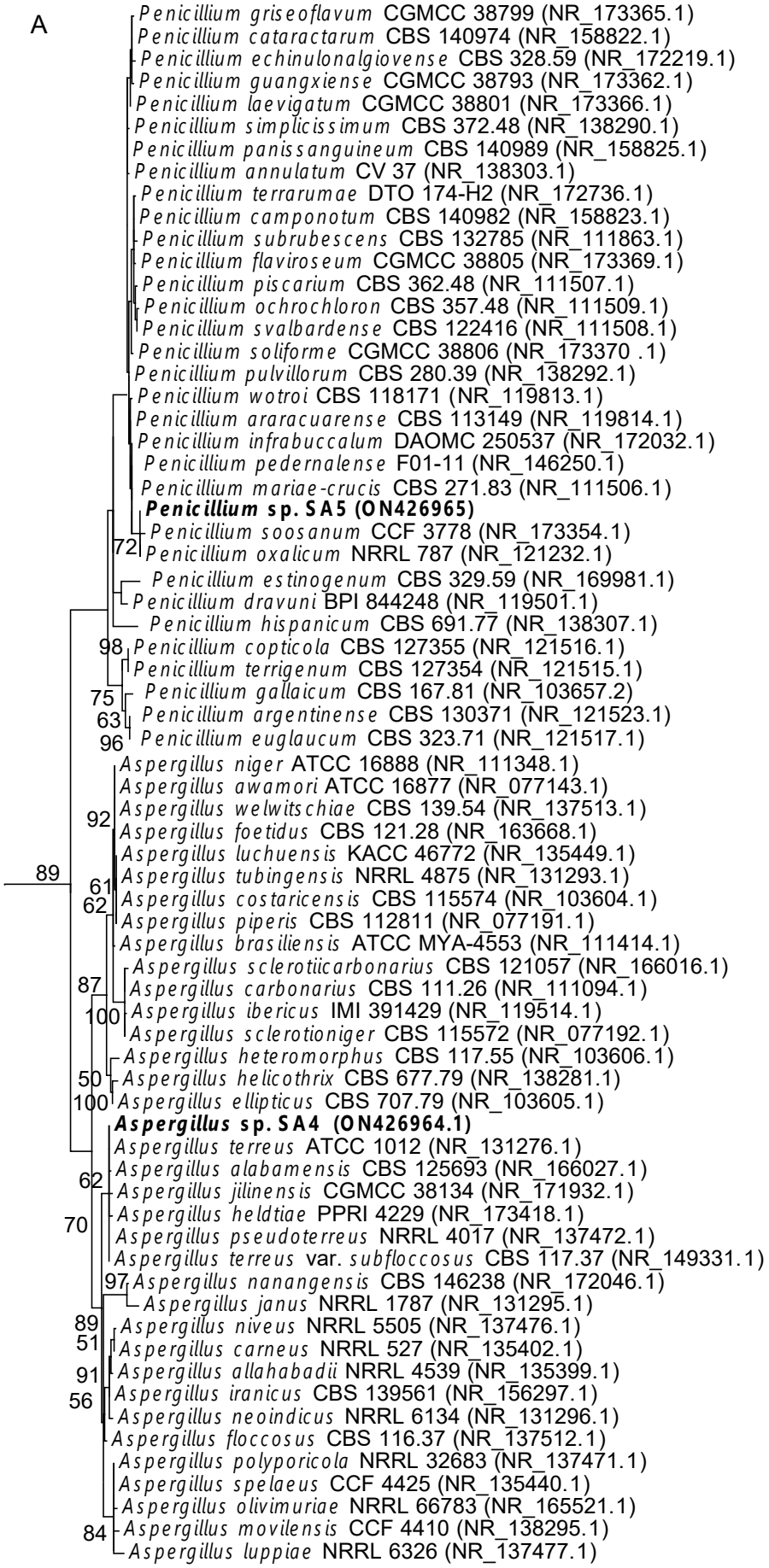
A
Penicillium griseoflavum CGMCC 38799 (NR_173365.1)
Penicillium cataractarum CBS 140974 (NR_158822.1)
Penicillium echinulonalgiovense CBS 328.59 (NR_172219.1)
Penicillium guangxiense CGMCC 38793 (NR_173362.1)
Penicillium laevigatum CGMCC 38801 (NR_173366.1)
Penicillium simplicissimum CBS 372.48 (NR_138290.1)
Penicillium panissanguineum CBS 140989 (NR_158825.1)
Penicillium annulatum CV 37 (NR_138303.1)
Penicillium terrarumae DTO 174-H2 (NR_172736.1)
Penicillium camponotum CBS 140982 (NR_158823.1)
Penicillium subrubescens CBS 132785 (NR_111863.1)
Penicillium flaviroseum CGMCC 38805 (NR_173369.1)
Penicillium piscarium CBS 362.48 (NR_111507.1)
Penicillium ochrochloron CBS 357.48 (NR_111509.1)
Penicillium svalbardense CBS 122416 (NR_111508.1)
Penicillium soliforme CGMCC 38806 (NR_173370 .1)
Penicillium pulvillorum CBS 280.39 (NR_138292.1)
Penicillium wotroi CBS 118171 (NR_119813.1)
Penicillium araracuarense CBS 113149 (NR_119814.1)
Penicillium infrabuccalum DAOMC 250537 (NR_172032.1)
Penicillium pedernalense F01-11 (NR_146250.1)
Penicillium mariae-crucis CBS 271.83 (NR_111506.1)
Penicillium sp. SA5 (ON426965)
Penicillium soosanum CCF 3778 (NR_173354.1)
72
Penicillium oxalicum NRRL 787 (NR_121232.1)
Penicillium estinogenum CBS 329.59 (NR_169981.1)
Penicillium dravuni BPI 844248 (NR_119501.1)
Penicillium hispanicum CBS 691.77 (NR_138307.1)
98
Penicillium copticola CBS 127355 (NR_121516.1)
Penicillium terrigenum CBS 127354 (NR_121515.1)
75
Penicillium gallaicum CBS 167.81 (NR_103657.2)
63
Penicillium argentinense CBS 130371 (NR_121523.1)
96
Penicillium euglaucum CBS 323.71 (NR_121517.1)
Aspergillus niger ATCC 16888 (NR_111348.1)
Aspergillus awamori ATCC 16877 (NR_077143.1)
92
Aspergillus welwitschiae CBS 139.54 (NR_137513.1)
Aspergillus foetidus CBS 121.28 (NR_163668.1)
Aspergillus luchuensis KACC 46772 (NR_135449.1)
89
Aspergillus tubingensis NRRL 4875 (NR_131293.1)
61
62
Aspergillus costaricensis CBS 115574 (NR_103604.1)
Aspergillus piperis CBS 112811 (NR_077191.1)
Aspergillus brasiliensis ATCC MYA-4553 (NR_111414.1)
Aspergillus sclerotiicarbonarius CBS 121057 (NR_166016.1)
87
Aspergillus carbonarius CBS 111.26 (NR_111094.1)
100
Aspergillus ibericus IMI 391429 (NR_119514.1)
Aspergillus sclerotioniger CBS 115572 (NR_077192.1)
Aspergillus heteromorphus CBS 117.55 (NR_103606.1)
50
Aspergillus helicothrix CBS 677.79 (NR_138281.1)
100
Aspergillus ellipticus CBS 707.79 (NR_103605.1)
Aspergillus sp. SA4 (ON426964.1)
Aspergillus terreus ATCC 1012 (NR_131276.1)
62
Aspergillus alabamensis CBS 125693 (NR_166027.1)
Aspergillus jilinensis CGMCC 38134 (NR_171932.1)
70
Aspergillus heldtiae PPRI 4229 (NR_173418.1)
Aspergillus pseudoterreus NRRL 4017 (NR_137472.1)
Aspergillus terreus var. subfloccosus CBS 117.37 (NR_149331.1)
97
Aspergillus nanangensis CBS 146238 (NR_172046.1)
Aspergillus janus NRRL 1787 (NR_131295.1)
89
Aspergillus niveus NRRL 5505 (NR_137476.1)
51
Aspergillus carneus NRRL 527 (NR_135402.1)
91
Aspergillus allahabadii NRRL 4539 (NR_135399.1)
56
Aspergillus iranicus CBS 139561 (NR_156297.1)
Aspergillus neoindicus NRRL 6134 (NR_131296.1)
Aspergillus floccosus CBS 116.37 (NR_137512.1)
Aspergillus polyporicola NRRL 32683 (NR_137471.1)
Aspergillus spelaeus CCF 4425 (NR_135440.1)
Aspergillus olivimuriae NRRL 66783 (NR_165521.1)
84
Aspergillus movilensis CCF 4410 (NR_138295.1)
Aspergillus luppiae NRRL 6326 (NR_137477.1)

293

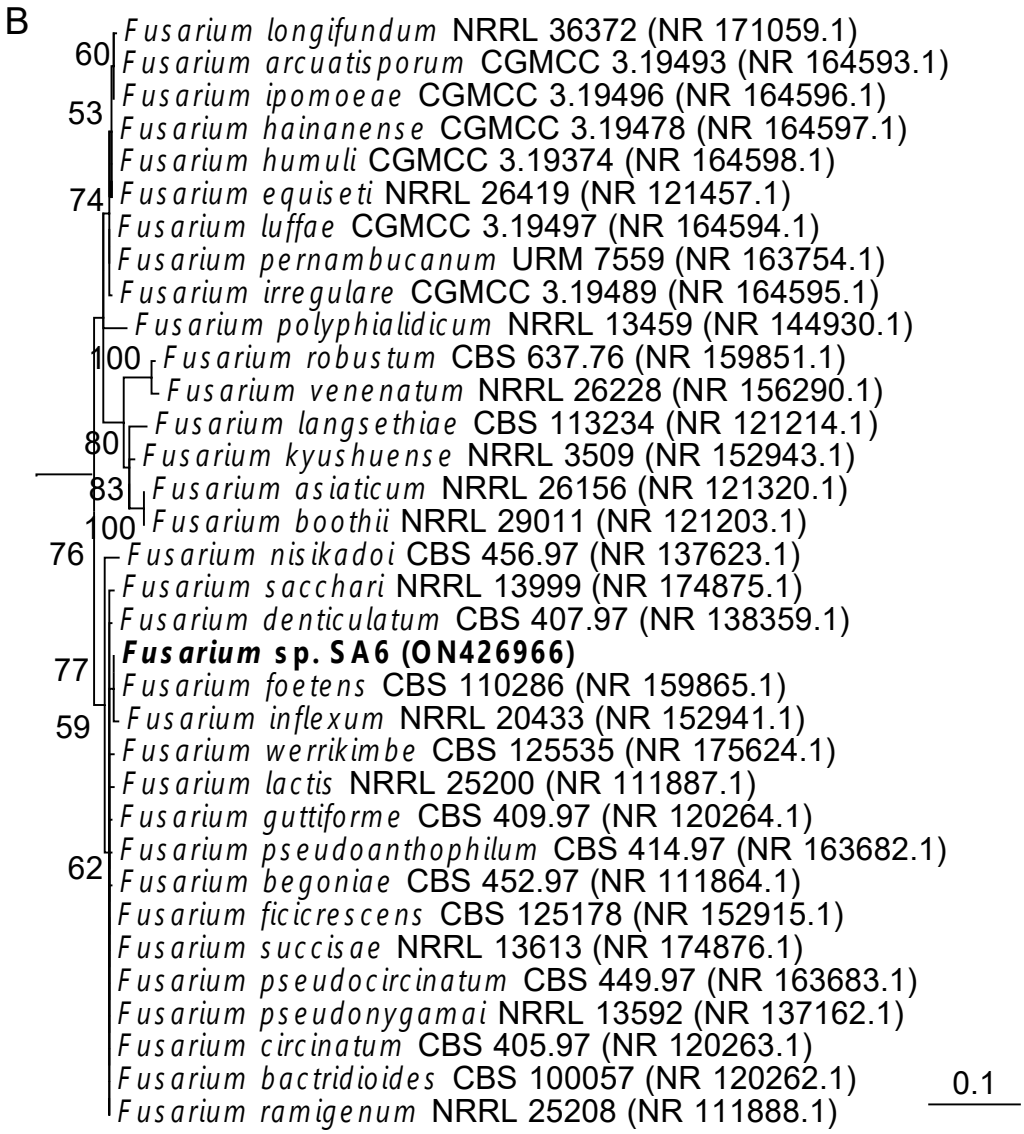

Figure S2: Phylogenetic placement of the three fungal strains SA4, SA5 and SA6 among the ITS region sequences of the next related fundal strains. Reference sequences were obtained by BLAST analysis in NCBI. The phylogenetic tree was constructed with the Maximum Likelihood method based on the Kimura 2-parameter model using MEGA7. The analysis involved 293 nucleotide sequences, the number of sequences in the depicted trees were reduced to the sequences which clustered directly with the SA strains. The tree was splitted in A: *Aspergillus/Penicillium* and B: *Fusarium* cluster. All positions with less than 95% site coverage were eliminated. There were a total of 389 positions in the final dataset. Numbers at nodes represent bootstrap values of 50% and higher based on 100 replications. Bar: 0.1 nucleotide substitutions per nucleotide sequence positions.

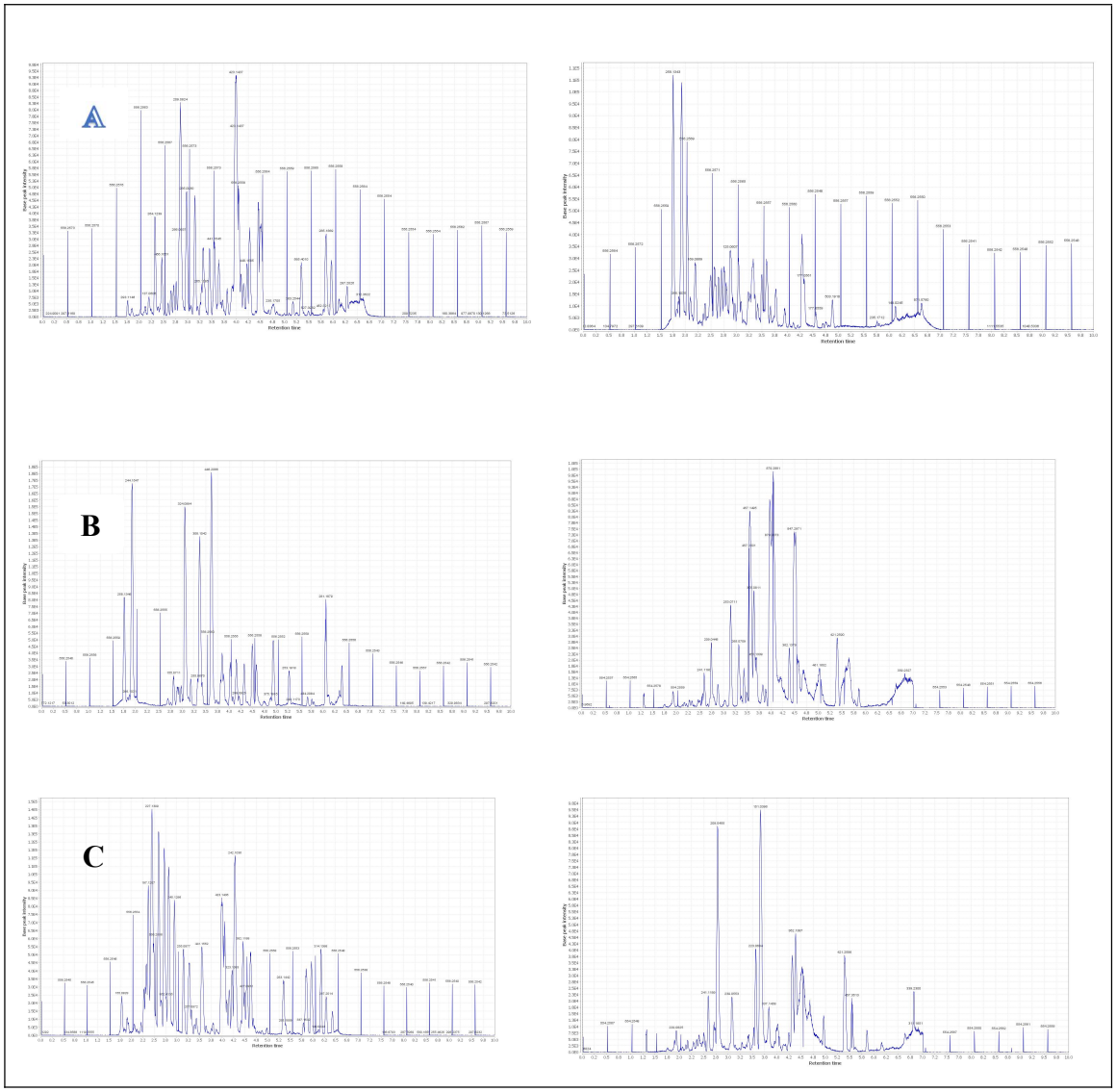

Figure S3. Total ion chromatogram of the crude extracts of strain SA4 (A), strain SA5 (B) and strain SA6 (C) cultured on PDA media in positive and negative ionization modes.

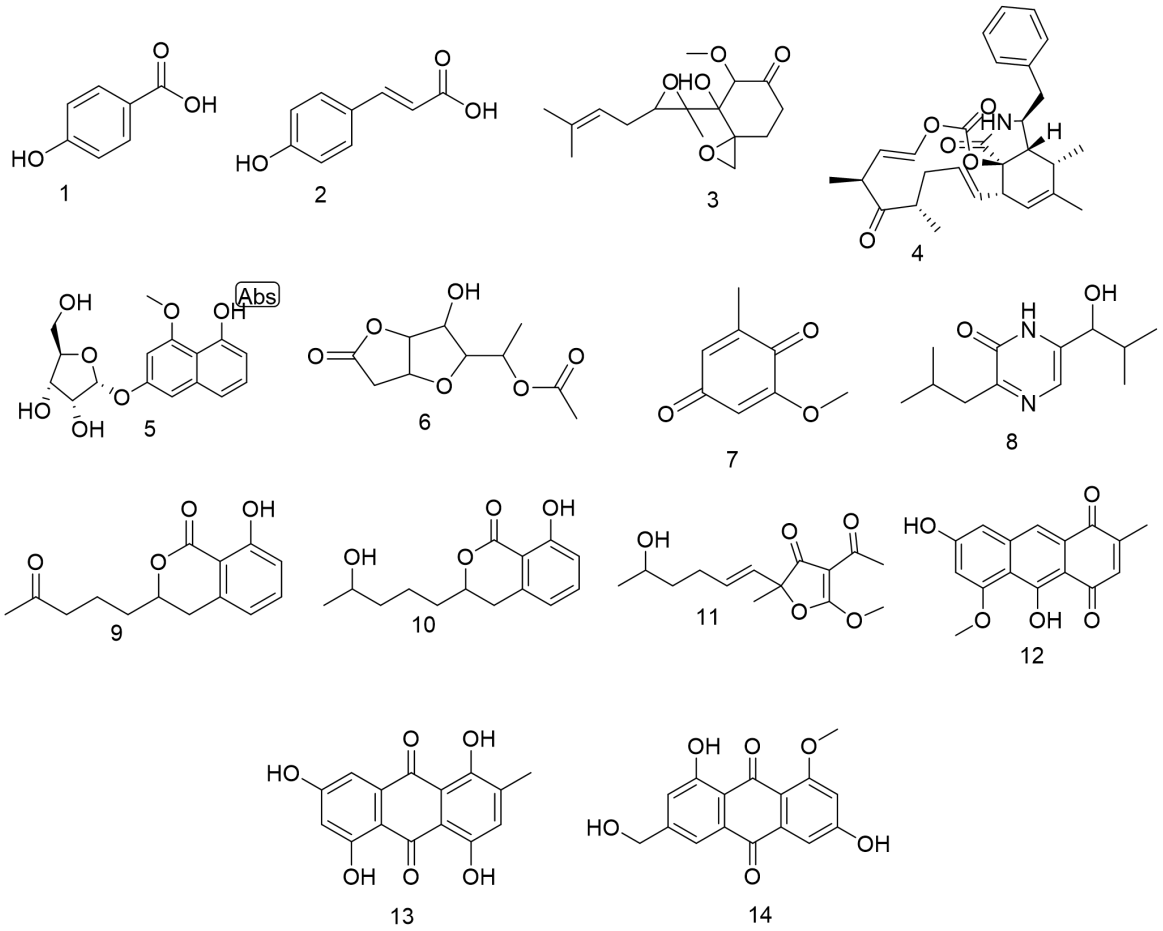

Figure S4. Chemical structures of the dereplicated metabolites from the extracts of strain SA4, strain SA5 and strain SA6.

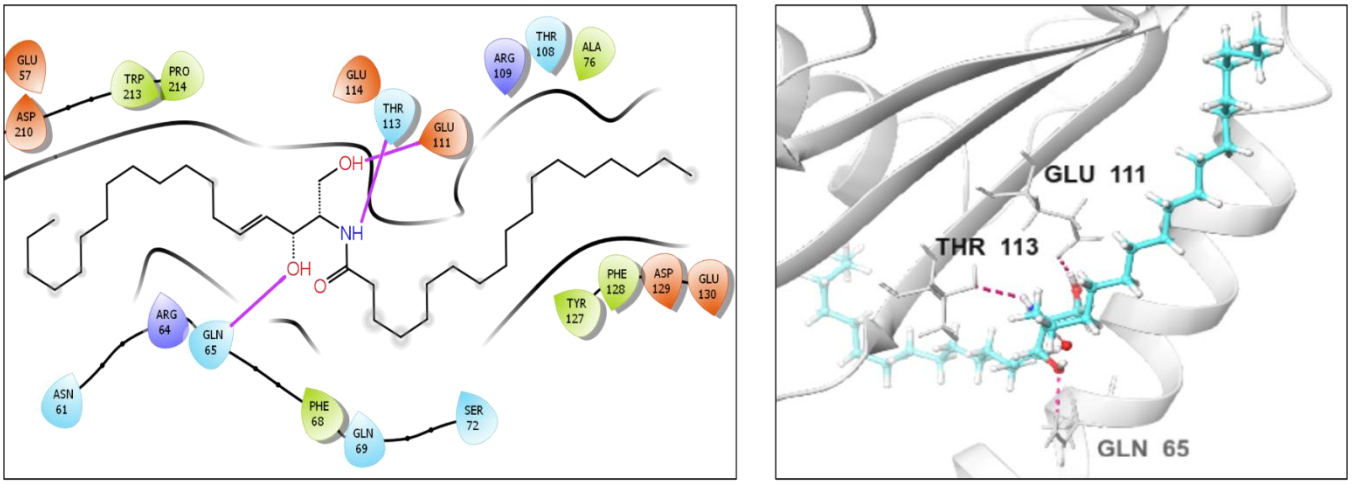

Figure S5. 2D & **3D** Views (A & B) of D-e-C18 ceramide docked in SET oncoprotein (pdb: 2E50)

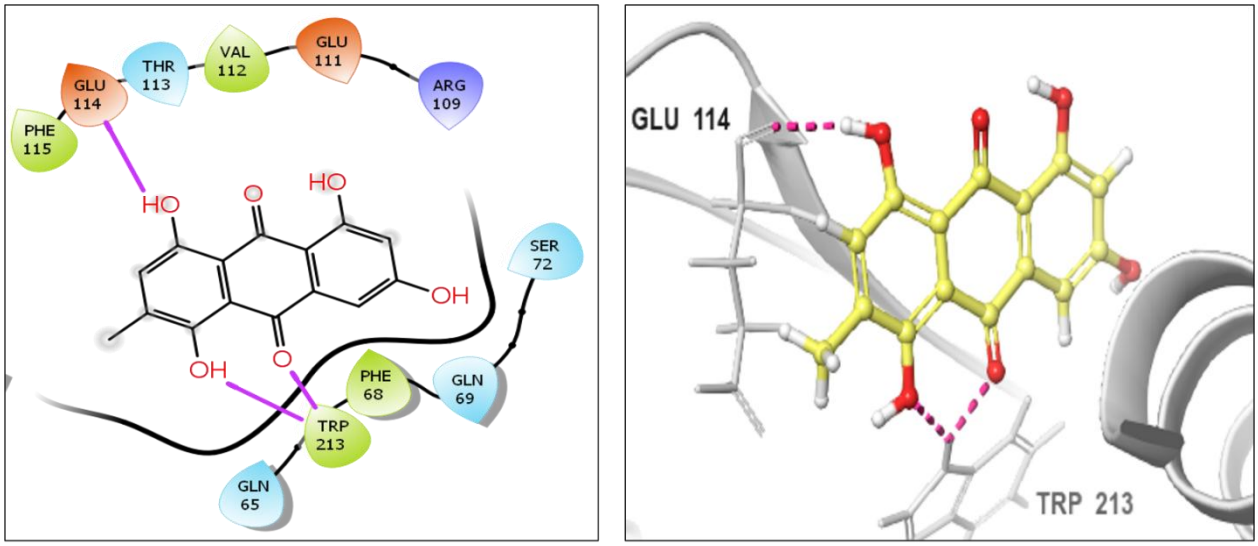

Figure S6. 2D & 3D Views (A & B) of catenarin docked in SET oncoprotein (pdb: 2E50)

References

Abdelmohsen UR, Szesny M, Othman EM, Schirmeister T, Grond S, Stopper H, Hentschel U. 2012. Antioxidant and anti-protease activities of diazepinomicin from the sponge-associated *Micromonospora* strain RV115. Marine drugs. 10(10):2208-2221.

Al Kazman BS, Prieto JM. 2021. Friends or Foes? Cytotoxicity, HPTLC and NMR Analyses of Some Important Naturally Occurring Hydroxyanthraquinones. Nutraceuticals. 1(1):13-30.

Anke H, Kolthoum I, Laatsch H. 1980. Metabolic products of microorganisms. 192. The anthraquinones of the *Aspergillus glaucus* group. II. Biological activity. Archives of Microbiology. 126(3):231-236.

Brase S, Encinas A, Keck J, Nising CF. 2009. Chemistry and biology of mycotoxins and related fungal metabolites. Chemical reviews. 109(9):3903-3990.

Cane DE, McIlwaine DB. 1987. The biosynthesis of ovalicin from β-trans-bergamotene. Tetrahedron letters. 28(52):6545-6548.

De Palma RM, Parnham SR, Li Y, Oaks JJ, Peterson YK, Szulc ZM, Roth BM, Xing Y, Ogretmen BJTFJ. 2019. The NMR-based characterization of the FTY720-SET complex reveals an alternative mechanism for the attenuation of the inhibitory SET-PP2A interaction. 33(6):7647-7666.

Gadallah M, Asaad NY, Shabaan M, Elkholy SS, Samara MY, Taie DJJoI, Immunochemistry. 2022. Role of SET oncoprotein in hepatocellular carcinoma: An immunohistochemical study.1-15.

Griffith EC, Su Z, Turk BE, Chen S, Chang Y-H, Wu Z, Biemann K, Liu JO. 1997. Methionine aminopeptidase (type 2) is the common target for angiogenesis inhibitors AGM-1470 and ovalicin. Chemistry & biology. 4(6):461-471.

Hall C. 2001. Sources of natural antioxidants: oilseeds, nuts, cereals, legumes, animal products and microbial sources. Antioxidants in food Practical Applications Pokorny, J, Yanishlieva, N y Gordon, M(Editores) CRC Woodhead Publishing Limited Cambrige, Inglaterra.

He J, Wijeratne EK, Bashyal BP, Zhan J, Seliga CJ, Liu MX, Pierson EE, Pierson LS, VanEtten HD, Gunatilaka AL. 2004. Cytotoxic and other metabolites of *Aspergillus* inhabiting the rhizosphere of Sonoran desert plants. Journal of natural products. 67(12):1985-1991.

Hisham M, Hassan HA, Gomaa HA, Youssif BG, Hayallah AM, Abdel-Aziz MJJoMS. 2022. Structure-based design, synthesis and antiproliferative action of new quizoline-4-one/chalcone hybrids as EGFR inhibitors.132422.

Innis MA, Gelfand DH, Sninsky JJ, White TJ. 2012. PCR protocols: a guide to methods and applications. Academic press.

Jaganathan SK, Supriyanto E, Mandal M. 2013. Events associated with apoptotic effect of p-Coumaric acid in HCT-15 colon cancer cells. World Journal of Gastroenterology: WJG. 19(43):7726.

Jiang W, Tian X, Wang Y, Sun Z, Dong P, Wang C, Huo X, Zhang B, Huang S, Deng S. 2016. The natural anthraquinones from *Rheum palmatum* induced the metabolic disorder of melatonin by inhibiting human CYP and SULT enzymes. Toxicology Letters. 262:27-38.

Jin L, Quan C, Hou X, Fan S. 2016. Potential pharmacological resources: Natural bioactive compounds from marine-derived fungi. Marine drugs. 14(4):76.

Kimura MJJome. 1980. A simple method for estimating evolutionary rates of base substitutions through comparative studies of nucleotide sequences. 16(2):111-120.

Kumar S, Stecher G, Tamura K. 2016. MEGA7: molecular evolutionary genetics analysis version 7.0 for bigger datasets. Molecular biology and evolution. 33(7):1870-1874.

Kushwaha M, Qayum A, Jain SK, Singh J, Srivastava AK, Srivastava S, Sharma N, Abrol V, Malik R, Singh SK. 2021. Tandem MS-Based Metabolite Profiling of 19, 20-Epoxycytochalasin C Reveals the Importance of a Hydroxy Group at the C7 Position for Biological Activity. ACS omega. 6(5):3717-3726.

Li Y-F, Wu X-B, Niaz S-I, Zhang L-H, Huang Z-J, Lin Y-C, Li J, Liu L. 2017. Effect of culture conditions on metabolites produced by the crinoid-derived fungus *Aspergillus ruber* 1017. Natural product research. 31(11):1299-1304.

Lin Z-J, Zhang G-J, Zhu T-J, Liu R, Wei H-J, Gu Q-Q. 2009. Bioactive Cytochalasins from *Aspergillus flavipes*, an Endophytic Fungus Associated with the Mangrove Plant *Acanthus ilicifolius* [10.1002/hlca.200800455]. Helv Chim Acta. 92(8):1538-1544.
Ludwig W, Strunk O, Westram R, Richter L, Meier H, Yadhukumar, Buchner A, Lai T, Steppi S, Jobb GJNar. 2004. ARB: a software environment for sequence data. 32(4):1363-1371.
Lv Q, Chang C, Li Y, Du Y, Liu J. 2020. Stereoselective synthesis of (−)-protulactone A. Tetrahedron. 76(26):131290.
Monchy S, Sanciu G, Jobard M, Rasconi S, Gerphagnon M, Chabé M, Cian A, Meloni D, Niquil N, Christaki UJEm. 2011. Exploring and quantifying fungal diversity in freshwater lake ecosystems using rDNA cloning/sequencing and SSU tag pyrosequencing. 13(6):1433-1453.
Pavithra N, Sathish L, Ananda K. 2012. Antimicrobial and enzyme activity of endophytic fungi isolated from Tulsi. Journal of Pharmaceutical and Biomedical Sciences (JPBMS). 16(16):2014.
Pharamat T, Palaga T, Piapukiew J, Whalley AJ, Sihanonth P. 2013. Antimicrobial and anticancer activities of endophytic fungi from *Mitrajyna javanica* Koord and Val. African Journal of Microbiology Research. 7(49):5565-5572.
Quast C, Pruesse E, Yilmaz P, Gerken J, Schweer T, Yarza P, Peplies J, Glöckner FOJNar. 2012. The SILVA ribosomal RNA gene database project: improved data processing and web-based tools. 41(D1):D590-D596.
Rasheed T, Bilal M, Iqbal HM, Li C. 2017. Green biosynthesis of silver nanoparticles using leaves extract of *Artemisia vulgaris* and their potential biomedical applications. Colloids and Surfaces B: Biointerfaces. 158:408-415.
Sayed AM, Sherif NH, El-Gendy AO, Shamikh YI, Ali AT, Attia EZ, El-Katatny MmH, Khalifa BA, Hassan HM, Abdelmohsen UR. 2020. Metabolomic profiling and antioxidant potential of three fungal endophytes derived from *Artemisia annua* and *Medicago sativa*. Natural Product Research.1-5.
Seidel C, Schnekenburger M, Dicato M, Diederich M. 2014. Antiproliferative and proapoptotic activities of 4-hydroxybenzoic acid-based inhibitors of histone deacetylases. Cancer letters. 343(1):134-146.
Shady NH, Abdelmohsen UR, AboulMagd AM, Amin MN, Ahmed S, Fouad MA, Kamel MSJNPR. 2021. Cytotoxic potential of the Red Sea sponge *Amphimedon* sp. supported by in silico modelling and dereplication analysis. 35(24):6093-6098.
Sohn J-H, Oh H-C. 2010. Protulactones A and B: two new polyketides from the marine-derived fungus *Aspergillus* sp. SF-5044. Bulletin of the Korean Chemical Society. 31(6):1695-1698.
Stott D, Martin J. 1989. Organic matter decomposition and retention in arid soils. Arid Land Research and Management. 3(2):115-148.
Tawfike AF, Romli M, Clements C, Abbott G, Young L, Schumacher M, Diederich M, Farag M, Edrada-Ebel R. 2019. Isolation of anticancer and anti-trypanosome secondary metabolites from the endophytic fungus *Aspergillus flocculus* via bioactivity guided isolation and MS based metabolomics. Journal of Chromatography B. 1106:71-83.
Wu Y, Chen Y, Huang X, Pan Y, Liu Z, Yan T, Cao W, She Z. 2018. α-Glucosidase inhibitors: diphenyl ethers and phenolic bisabolane sesquiterpenoids from the mangrove endophytic fungus *Aspergillus flavus* QQSG-3. Marine drugs. 16(9):307.
Ye K, Ai H-L, Liu J-K. 2021. Identification and Bioactivities of Secondary Metabolites Derived from Endophytic Fungi Isolated from Ethnomedicinal Plants of Tujia in Hubei Province: A Review. Natural Products and Bioprospecting.1-21.
Ying G, Yang L, van GEELEN L, EJIKEUGWU CP, ESIMONE CO, OKOYE FB, PROKSCH P, KALSCHEUER R. 2021. Secondary metabolites of a marine-derived *Penicillium ochrochloron*. Notulae Scientia Biologicae. 13(3):11020-11020.
Youssef FS, Singab ANB. 2021. An updated review on the secondary metabolites and biological activities of *Aspergillus ruber* and *Aspergillus flavus* and exploring the cytotoxic potential of their isolated compounds using virtual screening. Evidence-Based Complementary and Alternative Medicine. 2021.
Zhu W. 2018. Xiaoping Peng, Yi Wang, Tonghan Zhu. Arch Pharm Res. 41:184-191.